

# GoLF-NRT: Integrating Global Context and Local Geometry for Few-Shot View Synthesis\*

You Wang<sup>1†</sup> Li Fang<sup>1†</sup> Hao Zhu<sup>2</sup> Fei Hu<sup>1</sup> Long Ye<sup>1</sup> Zhan Ma<sup>2</sup>

<sup>1</sup>Key Laboratory of Media Audio and Video (Communication University of China),  
Ministry of Education, Beijing 100024, China

<sup>2</sup>School of Electronic Science and Engineering, Nanjing University, Nanjing 210023, China  
{wyou621, lifang8902, hufei, yelong}@cuc.edu.cn {zhuhao-photo, mazhan}@nju.edu.cn

## Abstract

Neural Radiance Fields (NeRF) have transformed novel view synthesis by modeling scene-specific volumetric representations directly from images. While generalizable NeRF models can generate novel views across unknown scenes by learning latent ray representations, their performance heavily depends on a large number of multi-view observations. However, with limited input views, these methods experience significant degradation in rendering quality. To address this limitation, we propose GoLF-NRT: a Global and Local feature Fusion-based Neural Rendering Transformer. GoLF-NRT enhances generalizable neural rendering from few input views by leveraging a 3D transformer with efficient sparse attention to capture global scene context. In parallel, it integrates local geometric features extracted along the epipolar line, enabling high-quality scene reconstruction from as few as 1 to 3 input views. Furthermore, we introduce an adaptive sampling strategy based on attention weights and kernel regression, improving the accuracy of transformer-based neural rendering. Extensive experiments on public datasets show that GoLF-NRT achieves state-of-the-art performance across varying numbers of input views, highlighting the effectiveness and superiority of our approach. Code is available at <https://github.com/KLMAV-CUC/GoLF-NRT>.

## 1. Introduction

Neural Radiance Fields (NeRF) [31] and its subsequent refinements [2–4, 42, 64] have achieved remarkable success in generating realistic, high-resolution, and view-consistent scenes for novel view synthesis. Despite these advancements, conventional NeRF approaches require expensive

\*This work is supported by National Key R&D Program of China under Grant No. 2021YFF0900500, and the National Natural Science Foundation of China under Grant No. 62001432.

<sup>†</sup>You Wang and Li Fang contributed equally to this work. Li Fang is the corresponding author.

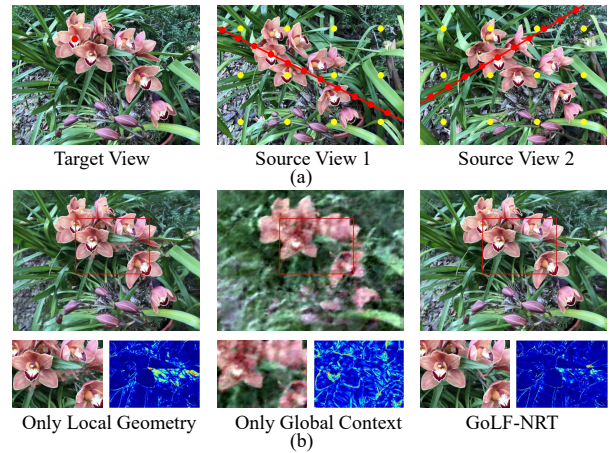


Figure 1. The integration of global context and local geometry in GoLF-NRT significantly enhances reconstruction accuracy. (a) Local geometric features (red) are extracted along the epipolar line of the target pixel, effectively capturing local geometric constraints, while surrounding features (yellow) provide the global context. (b) Relying solely on local features can introduce depth ambiguities and artifacts, while using only global features often fails to capture fine details. By combining both, GoLF-NRT achieves more precise and detailed reconstructions.

optimization with a large number captured images for each scene, hindering their widespread adoption in real-world applications. These constraints underscore the necessity of few-shot generalizable neural rendering, which aims to render unseen scenes from novel viewpoints using a limited number of input views.

To address the generalization issue, existing methods mainly introduce explicit or implicit priors to extract local geometrical features, such as the depth maps [12, 36], cost volumes [6, 55, 65], geometric consistency across views [1, 24, 33], and epipolar features encoded in attention maps [38, 39, 49]. However, these methods often require many input views to accurately capture geometry. With fewer views, they tend to produce over-smoothed textures or ar-

tifacts, particularly in occluded or reflective regions.

To address the few-shot issue, various types of auxiliary information have been incorporated with local geometrical features, including the normalization flow [66], semantic label constraints [15, 19] and frequency content [63]. However, these human-designed auxiliary features can only be reliably extracted with at least 3 views. When the number of input views further decreases, the inherent ambiguities in auxiliary information, such as large motion, incomplete semantic labels and restricted spectral bandwidth, exacerbate the over-smooth textures or artifacts in occlusion boundaries.

In this paper, we present GoLF-NRT (Global Local feature Fusion based Neural Rendering Transformer), a coarse-to-fine model that integrates global context features with enhanced local geometric features. Our model comprises two key modules: the global context feature extraction module and the local geometric feature extraction module. The global context feature extraction module employs a cross-view transformer-based encoder with multi-axis sparse attention to effectively learn the scene representation. This representation is then decoded into a global context feature for each ray, enabling the model to develop a comprehensive understanding of the scene from a limited set of viewpoints. The local geometric feature extraction module further refines this understanding by aggregating features along epipolar lines in each input view, alternating between a view transformer and a ray transformer. Unlike previous methods [51, 70] that directly fuse geometric and auxiliary features, our model uses the global context feature as a coarse prediction to better evaluate the contributions of different views. This approach ensures consistent scene understanding across views, improving the model’s ability to handle depth ambiguity and occlusions. Additionally, we introduce an adaptive sampling strategy that transforms attention weights [50] into a smooth, regularized probability density function (PDF) using kernel regression [44–46], thereby improving the model’s geometric perception and overall rendering quality.

Compared to prevailing methods such as [32, 38, 49, 70], our GoLF-NRT framework stands out by synthesizing target rays through the integration of global context understanding and local geometric perception. This distinctive combination enables our approach to perform exceptionally well in both many-shot and few-shot scenarios, offering a robust and versatile solution to the challenges of neural rendering across varying input conditions. Our main contributions are summarized as follows:

- We propose GoLF-NRT, a generalizable neural rendering technique that integrates global context with local geometry, ensuring consistent scene understanding across views and enhances the handling of depth ambiguity and occlusions.

- We introduce an adaptive sampling strategy using attention mechanisms and kernel regression to extract precise local geometric features, improving the model’s ability to accurately perceive geometry.
- Through extensive experiments and comparisons with state-of-the-art methods, we demonstrate that our framework consistently outperforms current generalizable neural rendering methods across various datasets, particularly in scenarios with limited input data.

## 2. Related Works

**NeRF and Generalizable NeRF.** NeRF [31] reconstructs images by predicting point density and color within a radiance field based on spatial coordinates and viewing directions. Follow-up works have improved rendering quality [2–4, 17], increased speed [7, 9, 16, 34, 40, 64], and enabled editing [27, 41, 52, 58, 61]. However, NeRF’s scene-specific implicit functions limit generalization. Generalizable NeRFs address this by encoding features at each 3D point and decoding them into volume density and radiance, allowing cross-scene generalization without retraining [6, 8, 29, 47, 60, 65]. Recently, attention mechanisms and transformers have further advanced novel view synthesis and generalization [10, 18, 21, 25, 35, 53, 62]. IBRNet [55] uses transformers for volumetric density prediction, while other methods [11, 23, 37, 38, 49] employ fully attention-based models for scene representation and ray color estimation. EVE-NeRF [32] enhances representation quality by integrating view and epipolar information, though it may struggle in few-shot scenarios due to data limitations and boundary artifacts.

**Few-shot Generalizable NeRF.** Various NeRF approaches address the few-shot problem. WaH-NeRF [1] tackles sample-position confusion with a deformable sampling strategy and mutual information loss. RegNeRF [33] regularizes color predictions for unseen viewpoints using a pre-trained flow model, integrating prior information for improved results. Other methods [12, 24, 36, 54, 59, 63, 66] enhance reconstruction by combining different modalities like geometry, depth, and frequency content. CaesarNeRF [70] utilize global average pooling to encode semantic information. However, it applies the same semantics to all rays, which can lead to conflicts, requiring additional calibration. LVSM [20] introduces a scalable, transformer-based model for view synthesis from sparse inputs that relies entirely on data-driven methods, bypassing traditional 3D biases.

**Generalizable 3D Gaussian Splatting.** Recent developments in generalizable Gaussian splatting methods have markedly improved the efficiency of novel view synthe-

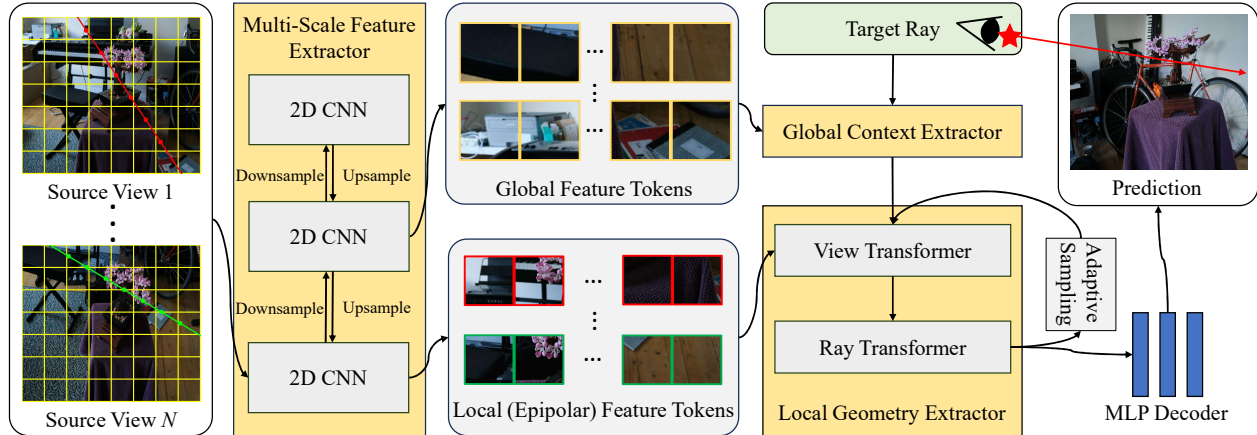


Figure 2. Overview of GoLF-NRT: 1) A FPN extracts multi-scale features from input views. 2) Coarse features are encoded to create scene representations, from which global context features are decoded for each target ray. 3) These global context features query local geometric features along the epipolar lines of all source views. The global and local features are concatenated and processed to predict the final target ray representation. 4) Pixel colors are directly predicted using a MLP.

sis. These methods bypass the need for per-scene optimization by directly regressing Gaussian parameters via a feed-forward architecture. For instance, PixelSplat [5] utilizes an epipolar transformer to resolve scale ambiguity and encode features, though its design is limited to image pair inputs. GPS-Gaussian [68] extends this approach to stereo matching, incorporating epipolar rectification, disparity estimation, and feature encoding. However, its reliance on ground-truth depth maps restricts its applicability. Splatter Image [43] proposes a single-view reconstruction approach based on Gaussian splatting, though its focus on object-centric reconstruction constrains its generalization to unseen scenes. MVSGaussian [28] combines multi-view stereo with a generalizable 3D Gaussian representation for real-time novel view synthesis. However, its single-sample-per-ray strategy necessitates highly accurate depth estimations, hindering its performance in complex scenes.

### 3. Methodology

Given a set of posed source views of an unknown scene, our goal is to synthesize novel views from arbitrary positions and directions. The proposed GoLF-NRT framework consists of two main stages: 1) constructing a coarse scene representation using global context, and 2) refining this representation by incorporating local geometry through epipolar feature aggregation. As shown in Fig. 2, we begin by extracting multi-scale features from source views. Coarse features, with larger receptive fields, are aggregated to capture global context, forming a preliminary target ray representation. This initial representation is then refined by aggregating fine features with smaller receptive fields along epipolar lines from all source views, resulting in a geometry-aware target ray representation. Finally, a multi-layer perceptron

(MLP) decoder predicts the target ray’s color.

#### 3.1. Multi-Scale Feature Extraction

Given  $N$  source views  $\{\mathbf{I}_i\}_{i=1}^N$  with camera parameters  $\{\mathbf{P}_i\}_{i=1}^N$ , we employ a feature pyramid network (FPN) [26] with shared weights to extract multi-scale features at 1/4, 1/8 and 1/16 resolutions. Unlike previous methods that operate on a single scale [32, 49, 70], our approach leverages features across multiple scales, thereby improving the representational capability of the model. Specifically, we use the 1/8-resolution features for global context extraction, while the 1/4-resolution features for capturing local geometric information.

#### 3.2. Global Context Feature Extraction

Both cost volume-based [21] and attention mechanism-based [32, 38] novel view synthesis methods focus heavily on local geometric reasoning for scene generalization but often lack a global perceptual framework, limiting their performance, particularly with a limited number of input views. This limitation arises from their reliance on features along epipolar lines, overlooking rich contextual information from other areas of the source views.

To address this, we propose incorporating features from all source views to create a global context feature for each ray. As described in Sec. 3.1, the encoder aggregates 1/8 resolution features from all source views, generating an implicit scene representation [37], denoted as  $\mathbf{Z}_g$ . However, this approach is computationally intensive and impractical for high-resolution rendering. To address this, we propose a 3D transformer incorporating sparse attention, as illustrated in Fig. 3.

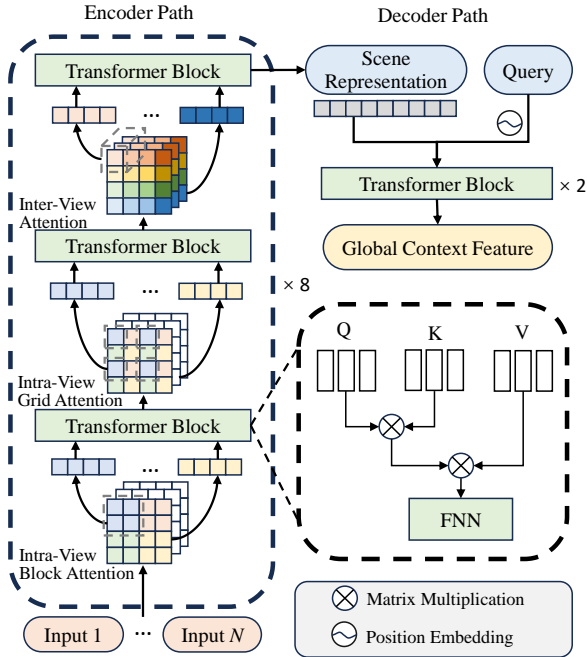


Figure 3. Network architecture of Global Context Feature Extraction Module. The 3D transformer, with near-linear complexity, encodes the scene into a scene representation, while the decoder generates the global context feature for each target ray.

**Near-Linear Complexity 3D Transformer.** Directly applying transformers to multi-view, high-resolution images is computationally expensive. To mitigate this, we adopt the sparse attention mechanism from MaxViT [48] and design a 3D transformer with near-linear computational complexity. Full-scale attention is decomposed into three sparse forms: intra-view block attention, intra-view grid attention, and inter-view attention. Intra-view block attention partitions each feature map of shape  $H \times W \times C$  into non-overlapping windows of size  $P \times P$ , reshaping it into a tensor of shape  $(\frac{H}{P} \times \frac{W}{P}, P \times P, C)$ , and applies self-attention within each window. Similarly, intra-view grid attention divides the tensor into a shape  $(G \times G, \frac{H}{G} \times \frac{W}{G}, C)$  using a fixed  $G \times G$  uniform grid, resulting in windows with an adaptive size  $\frac{H}{G} \times \frac{W}{G}$ , and applies self-attention along the grid axis  $G \times G$ . Finally, inter-view attention gathers feature maps from the  $N$  source views into a tensor of shape  $(N, H \times W, C)$ , and applies self-attention along the view axis  $N$ . By stacking these attention mechanisms sequentially, we capture both local and global interactions within each block. Notably, both intra-view block attention and intra-view grid attention operate with linear complexity relative to the input size, and the number of views  $N$  is typically small. As a result, this design achieves efficient global interaction without incurring the quadratic computational

costs of full-scale attention.

To generate the global context feature  $F_g$  for each target ray, we use a standard decoder transformer [50]. This decoder selectively attends to relevant features within the scene representation, providing a preliminary representation of the target ray. For a target ray  $r$  with specified origin and direction, the global context feature is computed by querying the decoder transformer  $\mathcal{D}$  as follows:

$$F_g = \mathcal{D}(r | Z_g). \quad (1)$$

In this mechanism, the target ray serves as the query for multi-head attention, while the keys and values are computed from the scene representation  $Z_g$ .

Through this interaction, the model selectively extracts the most relevant global context features for the target ray. This offers a comprehensive understanding of the entire scene, allowing the model to more effectively identify crucial changes in scene attributes, even when faced with diverse scenes or few input views.

### 3.3. Local Geometric Feature Extraction

This module constructs a coordinate-aligned feature volume from the  $1/4$ -resolution features  $\{F_i\}_{i=1}^N$  for the target ray, aiming to capture local geometry. We utilize GNT [49], a fully attention-based generalizable NeRF method, as our backbone. GNT aggregates features along epipolar lines in source views through two transformer-based stages. In the first stage, the view transformer predicts coordinate-aligned features for each point by aggregating information from the epipolar lines in the source views. This stage is designed to establish correspondences between queried points and the source views, providing a likelihood score that indicates the correlation of a pixel on the source view to the same point in 3D space without occlusion. Consequently, the output of the view transformer yields local geometric features of the pixels. In the second stage, the ray transformer aggregates these point-wise features along the ray to compute the ray color. However, while GNT performs well with a larger number of input views, it may encounter challenges when fewer views are available, primarily due to inconsistencies introduced by occlusion or reflections, which can compromise feature aggregation by the view transformer. To address these limitations, we propose two key improvements: global context-guided aggregation and adaptive sampling.

**Global Context-Guided Aggregation.** We enhance the view transformer by incorporating the global context feature  $F_g$  as the initial query, replacing the element-wise max pooling used in previous methods [49]:

$$F_l = \text{View-Transformer}(F_g | \{F_i, P_i\}_{i=1}^N), \quad (2)$$

where  $F_l$  denotes the local geometric feature. By leveraging the global context feature, which containing the most

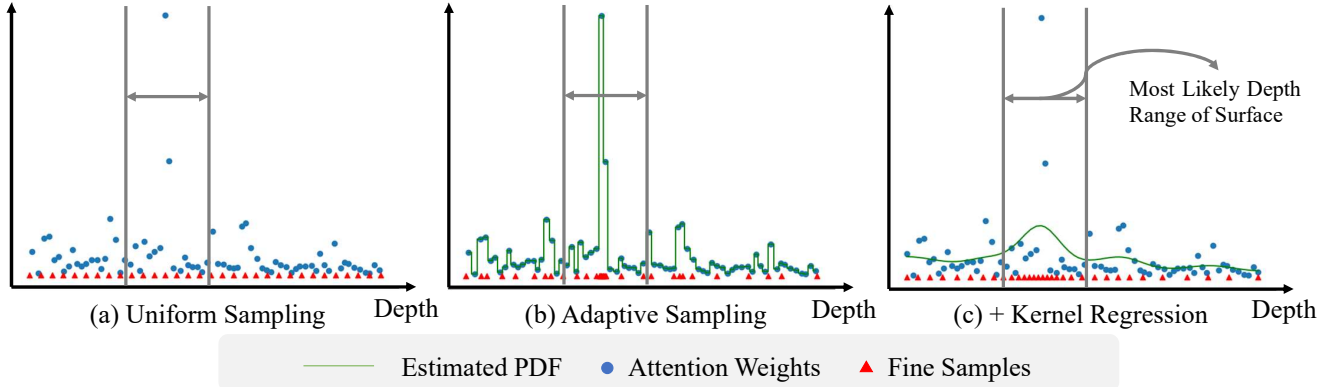


Figure 4. Illustration of how adaptive sampling with kernel regression enhances local geometric perception. (a) Uniform sampling, lacking surface depth constraints, distributes points broadly and randomly. (b) Adaptive sampling based solely on attention weights can lead to disorderly sampling due to the fundamental differences between feature similarity and the PDF used in volume rendering. (c) Our adaptive sampling with kernel regression bridges this gap, focusing samples within the most likely surface depth range, thereby improving subsequent image synthesis.

relevant information about the target ray in the scene representation  $\mathbf{Z}_g$ , the view transformer can more accurately assess contributions from various source views, resulting in more precise local geometric features  $\mathbf{F}_l$ . These local features are subsequently concatenated with the global context feature to create a global-local embedding:

$$\mathbf{F}_{g-l} = \mathbf{F}_g \oplus \mathbf{F}_l, \quad (3)$$

which is then aggregated by the ray transformer:

$$\mathbf{F}_r = \text{Ray-Transformer}(\mathbf{F}_{g-l}). \quad (4)$$

After iterating through 8 view and ray transformer blocks, we obtain the target ray representation  $\hat{\mathbf{F}}_r$ . These improvements enhance the robustness of our model in handling challenging scenarios with limited input views, significantly advancing the accuracy of local geometric feature extraction.

**Adaptive Sampling.** After the view transformer obtains point-wise features along the ray, the ray transformer aggregates them to form the ray color. The weighted aggregation can be regarded as an approximation of volume rendering [22], where the weights are learned through the attention mechanism. This insight inspires us to explore incorporating established volume rendering techniques to enhance modeling efficiency, such as hierarchical volume sampling, which prioritizes regions with significant contributions to the final rendering. We propose using the attention weights in the ray transformer as accumulation weights for volume rendering, similar to a probability density function (PDF). However, attention weights, derived from feature similarity, differ fundamentally from traditional PDFs used in volume rendering. As shown in Fig. 4(b), while attention weights

provide valuable cues, the estimated PDF can lead to disorderly sampling.

To bridge the gap between attention weights and the PDF, we introduce a kernel regression method [44–46] that transforms attention weights into a smooth, regularized PDF. Given  $N_c$  uniformly sampled depths  $\{d_i\}_{i=1}^{N_c}$  along the ray with corresponding attention weights  $\{w_i\}_{i=1}^{N_c}$ , the PDF at depth  $d$  is calculated as follows:

$$p(d) = \sum_{i=1}^{N_c} w_i * \frac{K(d, d_i)}{\sum_{i=1}^{N_c} K(d, d_i)}, \quad (5)$$

where  $K(d, d_i)$  is the Gaussian kernel:

$$K(d, d_i) = \frac{1}{h\sqrt{2\pi}} e^{-0.5\left(\frac{d-d_i}{h}\right)^2}, \quad (6)$$

and  $h$  is the bandwidth parameter. This method not only smooths the noise but also ensures that the resulting sampling distributions aligns with realistic, physically plausible shapes—either unimodal for opaque objects or multimodal for translucent materials, as depicted in Fig. 4(C).

In the uniform sampling stage,  $N_c$  features are uniformly sampled to estimate the PDF using Eq. (5). Subsequently,  $N_f$  refined feature locations are sampled from the PDF using inverse transform sampling, biasing the samples towards the object’s surface. In the adaptive sampling stage, all  $N_c + N_f$  samples are used. Both stages employ the same transformer.

### 3.4. MLP Decoder

Given the final feature of the target ray  $\hat{\mathbf{F}}_r$ , the ray color is then obtained through a multi-layer perceptron (MLP) decoder:

$$\hat{c} = \text{MLP}(\hat{\mathbf{F}}). \quad (7)$$

Input	Methods	LLFF			Blender			Shiny		
		PSNR $\uparrow$	SSIM $\uparrow$	LPIPS $\downarrow$	PSNR $\uparrow$	SSIM $\uparrow$	LPIPS $\downarrow$	PSNR $\uparrow$	SSIM $\uparrow$	LPIPS $\downarrow$
3-view	IBRNet [55]	23.00	0.752	0.262	22.44	0.874	0.195	21.96	0.710	0.281
	MVSNeRF [6]	19.84	0.729	0.314	23.62	0.897	0.176	18.55	0.645	0.343
	MatchNeRF [8]	22.30	0.731	0.234	23.20	0.897	0.164	20.77	0.672	0.249
	MVSGaussian [28]	24.07	0.857	0.164	<u>25.54</u>	<b>0.944</b>	<b>0.073</b>	20.49	0.661	0.254
	GNT [49]	23.28	0.768	0.230	<b>25.80</b>	0.905	0.104	22.47	0.720	0.247
	EVE-NeRF [32]	22.79	0.754	0.226	23.43	0.903	0.132	<u>24.11</u>	<b>0.781</b>	<b>0.204</b>
	CaesarNeRF [70]	<u>23.45</u>	<u>0.794</u>	<u>0.176</u>	23.56	0.908	0.131	22.74	0.723	0.241
	GoLF-NRT	<b>24.20</b>	<b>0.821</b>	<b>0.148</b>	24.30	<u>0.916</u>	<u>0.097</u>	<b>25.06</b>	<u>0.765</u>	<u>0.207</u>
2-view	MVSNeRF [6]	19.15	0.704	0.336	20.56	0.856	0.243	17.25	0.577	0.416
	MatchNeRF [8]	21.08	0.689	0.272	20.57	0.864	0.200	20.28	0.636	<u>0.278</u>
	pixelSplat [5]	<b>22.99</b>	<b>0.810</b>	<u>0.190</u>	15.77	0.755	0.314	-	-	-
	GNT [49]	20.94	0.687	0.301	<b>23.47</b>	0.877	<u>0.151</u>	20.42	0.617	0.327
	EVE-NeRF [32]	19.95	0.607	0.340	21.62	0.867	0.180	20.89	<u>0.667</u>	0.321
	CaesarNeRF [70]	21.94	0.736	0.224	22.07	<u>0.879</u>	0.176	<u>21.47</u>	0.652	0.293
	GoLF-NRT	<u>22.48</u>	<u>0.765</u>	<b>0.193</b>	<u>22.34</u>	<b>0.886</b>	<b>0.143</b>	<b>23.03</b>	<b>0.692</b>	<b>0.261</b>
	GNT [49]	16.60	0.491	0.514	15.53	0.634	0.371	15.99	0.400	0.548
1-view	CaesarNeRF [70]	<b>18.31</b>	<u>0.521</u>	<u>0.435</u>	<u>15.76</u>	<u>0.698</u>	<u>0.366</u>	<u>17.57</u>	<u>0.472</u>	<u>0.467</u>
	GoLF-NRT	<b>18.31</b>	<b>0.527</b>	<b>0.410</b>	<b>16.34</b>	<b>0.706</b>	<b>0.309</b>	<b>18.96</b>	<b>0.513</b>	<b>0.393</b>

Table 1. Quantitative comparison of state-of-the-art view synthesis methods on LLFF, Blender, and Shiny datasets with 1-3 input views. Best results are in bold, second-best are underlined.

## 4. Experiments

### 4.1. Settings

**Dataset.** Following [49, 55], we constructed our training data from both synthetic and real sources, including 1023 models from Google Scanned Object [13], RealEstate10K [69], Spaces scenes [14], and 102 real scenes captured with handheld cellphones [30, 55]. For evaluation, we used the LLFF [30], Blender [31], and Shiny [57] datasets. Notably, LLFF validation scenes were excluded from training, and Blender and Shiny datasets introduce significant variations in view distribution and scene content compared to the training dataset. The quality of the synthesized novel views is measured using the PSNR, SSIM [56], and LPIPS [67] metrics.

**Implementation Details.** GoLF-NRT is trained using the Mean Square Error (MSE) loss commonly used in NeRF [31]. We optimized the model end-to-end using the Adam optimizer, setting an initial learning rate of  $10^{-3}$  for the multi-scale feature extraction module and  $5 \times 10^{-4}$  for other modules, with exponential decay. Training ran for 250k iterations with 682 rays sampled per iteration. During uniform sampling, we used 128 samples per ray, with an additional 64 samples during adaptive sampling. Following [49], we construct source-target view pairs by selecting a target view and forming a pool of  $k \times N$  proximate views, where  $k \in (1, 3)$  and  $N \in (8, 12)$ . During training,  $k$  and  $N$  are uniformly sampled from these intervals, while  $N$  is fixed at 10 for evaluation to ensure consistency.

### 4.2. Comparative Studies

We compare GoLF-NRT with several state-of-the-art generalizable NeRF methods, including PixelNeRF [65], IBRNet [55], MVSNeRF [6], MatchNeRF [8], NeuRay [29], GPNR [38], GNT [49], CaesarNeRF [70], and EVE-NeRF [32]. We conducted experiments under both few-shot and many-shot configurations to provide a comprehensive comparison with existing methods, showcasing the broad applicability and superiority of GoLF-NRT.

As shown in Tab. 1, GoLF-NRT outperforms other methods across most metrics with 1 to 3 input views on LLFF, Blender, and Shiny. While all methods degrade with fewer views, our approach maintains high-quality results with minimal loss. Notably, with 3 input views on the LLFF dataset, GoLF-NRT surpasses CaesarNeRF [70] by 0.75 dB in PSNR, 0.027 in SSIM, and reduces LPIPS by 0.028. It’s also important to note that multi-view matching becomes irrelevant when only a single image is available, explaining why our results significantly outperform GNT [49]. While CaesarNeRF also leverages semantic information for few-shot novel view synthesis, it applies identical semantics to all rays, which can lead to conflicts, even with additional calibration. In contrast, our approach selectively extracts relevant global information for each ray, using it to guide local information extraction, thereby supporting accurate ray synthesis even on complex datasets such as Shiny dataset. With 1 input view on the Shiny dataset, GoLF-NRT improves over CaesarNeRF by 1.39 dB in PSNR, 0.041 in SSIM, and reduces LPIPS by 0.074.

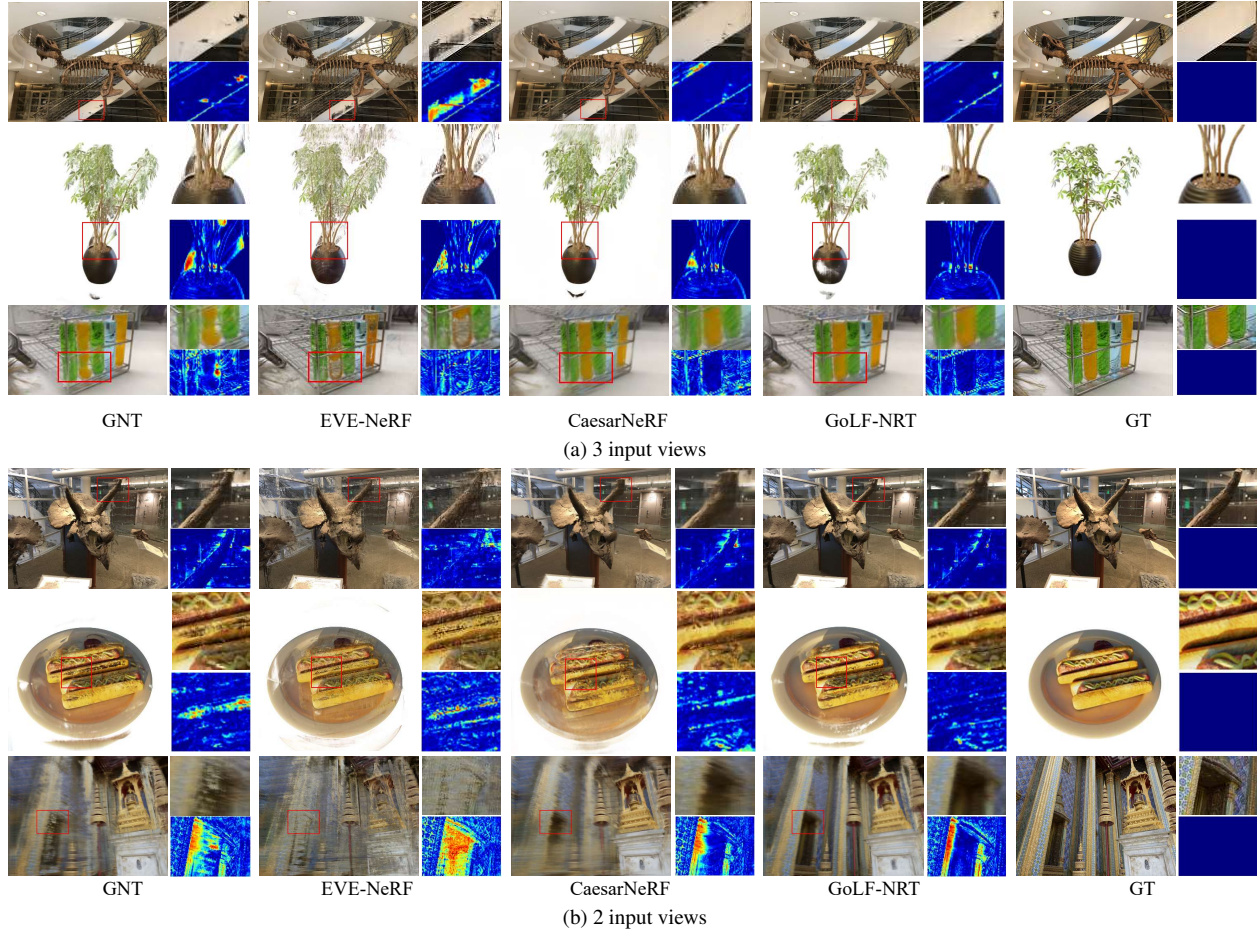


Figure 5. Qualitative comparison of GoLF-NRT with GNT, EVE-NeRF, and CaesarNeRF using 3 and 2 input views: (a) Trex scene (LLFF), Ficus scene (Blender), and Lab scene (Shiny); (b) Horns scene (LLFF), Hotdog scene (Blender), and Crest scene (Shiny). Each triplet shows the reconstructed image (left), a zoomed-in view (upper right), and its corresponding error map (lower right).

Fig. 5 presents qualitative results for configurations with 3 and 2 input views. It is evident that previous methods relying solely on local features for multi-view matching encounter difficulties in regions with edges, depth discontinuities, or reflections, often resulting in mismatches. By incorporating global features within the view transformer, our approach achieves a more holistic scene understanding, leading to enhanced consistency in matching across views.

We also demonstrate generalizable results under many-shot conditions (10-views), as shown in Tab. 2. Our method achieved the best or second-best results across all metrics. Fig. 6 provides a qualitative comparison, confirming its effectiveness in both few-shot and many-shot scenarios.

### 4.3. Ablations and Analysis

We conduct a series of ablation studies to evaluate the effectiveness of our design. Tab. 3 shows that our method, which integrates both global and local features, improves PSNR by 0.44 dB, underscoring the importance of global

context in achieving accurate novel view synthesis. Fig. 8 illustrates that our design effectively focuses on important regions. Adaptive sampling using kernel regression on attention weights reduces noise from local similarities and produces a more targeted sampling distribution, resulting in a 0.32 dB increase in PSNR. Fig. 7 shows that this significantly enhances depth recovery at object boundaries. Additionally, Tab. 4 shows that full-scale attention is computationally impractical, while our 3D transformer reduces costs, enabling high-resolution processing.

## 5. Conclusion

In this paper, we introduced GoLF-NRT, a novel neural rendering transformer that integrates global and local features to enhance view synthesis from few input views. Our approach utilizes a 3D transformer with efficient sparse attention for global context understanding and an adaptive sampling strategy for accurate local geometry perception, significantly improving rendering quality. Extensive exper-

Methods	LLFF			Blender			Shiny		
	PSNR $\uparrow$	SSIM $\uparrow$	LPIPS $\downarrow$	PSNR $\uparrow$	SSIM $\uparrow$	LPIPS $\downarrow$	PSNR $\uparrow$	SSIM $\uparrow$	LPIPS $\downarrow$
PixelNeRF [65]	18.66	0.588	0.463	22.65	0.808	0.202	-	-	-
IBRNet [55]	25.17	0.813	0.200	26.73	0.908	0.101	23.60	0.785	0.180
NeuRay [29]	25.35	0.818	0.198	26.48	0.944	0.091	25.72	0.880	0.175
GPNR [38]	25.72	<b>0.880</b>	0.175	<u>28.29</u>	0.927	0.080	24.12	0.860	0.170
GNT [49]	25.53	0.836	0.178	26.01	0.925	0.088	26.56	0.852	0.132
CaesarNeRF [70]	25.16	0.851	<u>0.138</u>	26.75	0.915	0.083	26.66	0.849	0.146
EVE-NeRF [32]	<b>27.16</b>	0.869	0.141	27.03	<u>0.952</u>	<u>0.072</u>	<u>27.41</u>	<u>0.883</u>	<u>0.113</u>
GoLF-NRT	<u>26.42</u>	<u>0.879</u>	<b>0.109</b>	<b>29.74</b>	<b>0.963</b>	<b>0.060</b>	<b>28.01</b>	<b>0.885</b>	<b>0.112</b>

Table 2. Quantitative comparison with state-of-the-art view synthesis methods on LLFF, Blender and Shiny datasets with 10 input views. Best results are in bold, second-best are underlined.

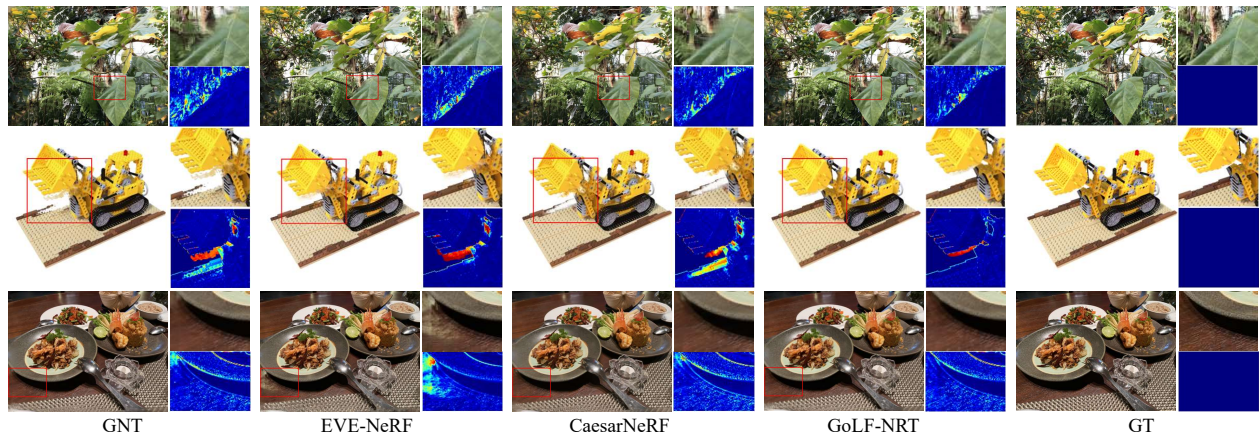


Figure 6. Qualitative comparison of GoLF-NRT with GNT, EVE-NeRF, and CaesarNeRF using 10 input views. Rows correspond to the Leaves scene (LLFF), Lego scene (Blender), and Food scene (Shiny). Each triplet includes a reconstructed image (left), a zoomed-in view (upper right), and its error map (lower right).

Model	PSNR $\uparrow$	SSIM $\uparrow$	LPIPS $\downarrow$
only local geometry	23.28	0.768	0.230
+ global context	23.55	0.791	0.170
+ global context as query	23.72	0.804	0.159
+ adaptive sampling	23.88	0.806	0.157
+ kernel regression	<b>24.20</b>	<b>0.821</b>	<b>0.148</b>

Table 3. Ablations. We trained model variants using the previously described setup and evaluated them on the LLFF dataset with 3 input views.

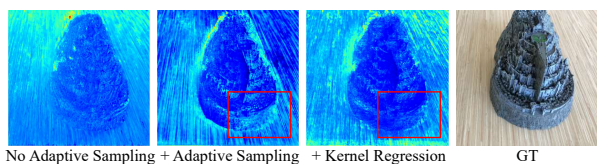


Figure 7. The depth maps from three sampling strategies show that adaptive sampling with kernel regression significantly improves accuracy, especially at boundaries with depth discontinuities.



Figure 8. Visualization of global and local attentions.

	FLOPs (G)	Parameters (M)
Full Attention	11.67	0.37
Our 3D Transformer	1.88	0.33

Table 4. Comparison of efficiency with full-scale attention.

iments demonstrated that GoLF-NRT achieves state-of-the-art performance across various datasets, particularly in scenarios with limited input views. Our method’s ability to handle depth ambiguity and occlusions highlights its robustness and versatility, making it a promising solution for real-world applications in neural rendering.

## References

- [1] Yanqi Bao, Yuxin Li, Jing Huo, Tianyu Ding, Xinyue Liang, Wenbin Li, and Yang Gao. Where and how: Mitigating confusion in neural radiance fields from sparse inputs. In *Proceedings of the 31st ACM International Conference on Multimedia*, pages 2180–2188, 2023.
- [2] Jonathan T Barron, Ben Mildenhall, Matthew Tancik, Peter Hedman, Ricardo Martin-Brualla, and Pratul P Srinivasan. Mip-nerf: A multiscale representation for anti-aliasing neural radiance fields. In *Proceedings of the IEEE/CVF international conference on computer vision*, pages 5855–5864, 2021.
- [3] Jonathan T Barron, Ben Mildenhall, Dor Verbin, Pratul P Srinivasan, and Peter Hedman. Mip-nerf 360: Unbounded anti-aliased neural radiance fields. In *Proceedings of the IEEE/CVF conference on computer vision and pattern recognition*, pages 5470–5479, 2022.
- [4] Jonathan T Barron, Ben Mildenhall, Dor Verbin, Pratul P Srinivasan, and Peter Hedman. Zip-nerf: Anti-aliased grid-based neural radiance fields. In *Proceedings of the IEEE/CVF International Conference on Computer Vision*, pages 19697–19705, 2023.
- [5] David Charatan, Sizhe Lester Li, Andrea Tagliasacchi, and Vincent Sitzmann. pixelsplat: 3d gaussian splats from image pairs for scalable generalizable 3d reconstruction. In *Proceedings of the IEEE/CVF Conference on Computer Vision and Pattern Recognition*, pages 19457–19467, 2024.
- [6] Anpei Chen, Zexiang Xu, Fuqiang Zhao, Xiaoshuai Zhang, Fanbo Xiang, Jingyi Yu, and Hao Su. Mvsnerf: Fast generalizable radiance field reconstruction from multi-view stereo. In *Proceedings of the IEEE/CVF international conference on computer vision*, pages 14124–14133, 2021.
- [7] Anpei Chen, Zexiang Xu, Andreas Geiger, Jingyi Yu, and Hao Su. Tensorf: Tensorial radiance fields. In *European conference on computer vision*, pages 333–350. Springer, 2022.
- [8] Yuedong Chen, Haofei Xu, Qianyi Wu, Chuanxia Zheng, Tat-Jen Cham, and Jianfei Cai. Explicit correspondence matching for generalizable neural radiance fields. *arXiv preprint arXiv:2304.12294*, 2023.
- [9] Zhiqin Chen, Thomas Funkhouser, Peter Hedman, and Andrea Tagliasacchi. Mobilenerf: Exploiting the polygon rasterization pipeline for efficient neural field rendering on mobile architectures. In *Proceedings of the IEEE/CVF Conference on Computer Vision and Pattern Recognition*, pages 16569–16578, 2023.
- [10] Julian Chibane, Aayush Bansal, Verica Lazova, and Gerard Pons-Moll. Stereo radiance fields (srf): Learning view synthesis for sparse views of novel scenes. In *Proceedings of the IEEE/CVF Conference on Computer Vision and Pattern Recognition*, pages 7911–7920, 2021.
- [11] Wenyan Cong, Hanxue Liang, Peihao Wang, Zhiwen Fan, Tianlong Chen, Mukund Varma, Yi Wang, and Zhangyang Wang. Enhancing nerf akin to enhancing llms: Generalizable nerf transformer with mixture-of-view-experts. In *Proceedings of the IEEE/CVF International Conference on Computer Vision*, pages 3193–3204, 2023.
- [12] Kangle Deng, Andrew Liu, Jun-Yan Zhu, and Deva Ramanan. Depth-supervised nerf: Fewer views and faster training for free. In *Proceedings of the IEEE/CVF Conference on Computer Vision and Pattern Recognition*, pages 12882–12891, 2022.
- [13] Laura Downs, Anthony Francis, Nate Koenig, Brandon Kinman, Ryan Hickman, Krista Reymann, Thomas B McHugh, and Vincent Vanhoucke. Google scanned objects: A high-quality dataset of 3d scanned household items. In *2022 International Conference on Robotics and Automation (ICRA)*, pages 2553–2560. IEEE, 2022.
- [14] John Flynn, Michael Broxton, Paul Debevec, Matthew Duvall, Graham Fyffe, Ryan Overbeck, Noah Snavely, and Richard Tucker. Deepview: View synthesis with learned gradient descent. In *Proceedings of the IEEE/CVF Conference on Computer Vision and Pattern Recognition*, pages 2367–2376, 2019.
- [15] Yiming Gao, Yan-Pei Cao, and Ying Shan. Surfelferf: Neural surfel radiance fields for online photorealistic reconstruction of indoor scenes. In *Proceedings of the IEEE/CVF Conference on Computer Vision and Pattern Recognition*, pages 108–118, 2023.
- [16] Peter Hedman, Pratul P Srinivasan, Ben Mildenhall, Jonathan T Barron, and Paul Debevec. Baking neural radiance fields for real-time view synthesis. In *Proceedings of the IEEE/CVF international conference on computer vision*, pages 5875–5884, 2021.
- [17] Wenbo Hu, Yuling Wang, Lin Ma, Bangbang Yang, Lin Gao, Xiao Liu, and Yuewen Ma. Tri-miprf: Tri-mip representation for efficient anti-aliasing neural radiance fields. In *Proceedings of the IEEE/CVF International Conference on Computer Vision*, pages 19774–19783, 2023.
- [18] Xin Huang, Qi Zhang, Ying Feng, Xiaoyu Li, Xuan Wang, and Qing Wang. Local implicit ray function for generalizable radiance field representation. In *Proceedings of the IEEE/CVF Conference on Computer Vision and Pattern Recognition*, pages 97–107, 2023.
- [19] Ajay Jain, Matthew Tancik, and Pieter Abbeel. Putting nerf on a diet: Semantically consistent few-shot view synthesis. In *Proceedings of the IEEE/CVF International Conference on Computer Vision*, pages 5885–5894, 2021.
- [20] Haian Jin, Hanwen Jiang, Hao Tan, Kai Zhang, Sai Bi, Tianyuan Zhang, Fujun Luan, Noah Snavely, and Zexiang Xu. Lvsm: A large view synthesis model with minimal 3d inductive bias, 2024.
- [21] Mohammad Mahdi Johari, Yann Lepoittevin, and François Fleuret. Geonerf: Generalizing nerf with geometry priors. In *Proceedings of the IEEE/CVF Conference on Computer Vision and Pattern Recognition*, pages 18365–18375, 2022.
- [22] James T Kajiya and Brian P Von Herzen. Ray tracing volume densities. *ACM SIGGRAPH computer graphics*, 18(3):165–174, 1984.
- [23] Jonáš Kulháněk, Erik Derner, Torsten Sattler, and Robert Babuška. Viewformer: Nerf-free neural rendering from few images using transformers. In *European Conference on Computer Vision*, pages 198–216. Springer, 2022.

- [24] Min-Seop Kwak, Jiuhn Song, and Seungryong Kim. Geconerf: Few-shot neural radiance fields via geometric consistency. *arXiv preprint arXiv:2301.10941*, 2023.
- [25] Jiaxin Li, Zijian Feng, Qi She, Henghui Ding, Changhu Wang, and Gim Hee Lee. Mine: Towards continuous depth mpi with nerf for novel view synthesis. In *Proceedings of the IEEE/CVF International Conference on Computer Vision*, pages 12578–12588, 2021.
- [26] Tsung Yi Lin, Piotr Dollar, Ross Girshick, Kaiming He, Bharath Hariharan, and Serge Belongie. Feature pyramid networks for object detection. *IEEE Computer Society*, 2017.
- [27] Steven Liu, Xiuming Zhang, Zhoutong Zhang, Richard Zhang, Jun-Yan Zhu, and Bryan Russell. Editing conditional radiance fields. In *Proceedings of the IEEE/CVF international conference on computer vision*, pages 5773–5783, 2021.
- [28] Tianqi Liu, Guangcong Wang, Shoukang Hu, Liao Shen, Xinyi Ye, Yuhang Zang, Zhiguo Cao, Wei Li, and Ziwei Liu. Mvsgaussian: Fast generalizable gaussian splatting reconstruction from multi-view stereo. In *European Conference on Computer Vision*, pages 37–53. Springer, 2024.
- [29] Yuan Liu, Sida Peng, Lingjie Liu, Qianqian Wang, Peng Wang, Christian Theobalt, Xiaowei Zhou, and Wenping Wang. Neural rays for occlusion-aware image-based rendering. In *Proceedings of the IEEE/CVF Conference on Computer Vision and Pattern Recognition*, pages 7824–7833, 2022.
- [30] Ben Mildenhall, Pratul P Srinivasan, Rodrigo Ortiz-Cayon, Nima Khademi Kalantari, Ravi Ramamoorthi, Ren Ng, and Abhishek Kar. Local light field fusion: Practical view synthesis with prescriptive sampling guidelines. *ACM Transactions on Graphics (TOG)*, 38(4):1–14, 2019.
- [31] Ben Mildenhall, Pratul P Srinivasan, Matthew Tancik, Jonathan T Barron, Ravi Ramamoorthi, and Ren Ng. Nerf: Representing scenes as neural radiance fields for view synthesis. *Communications of the ACM*, 65(1):99–106, 2021.
- [32] Zhiyuan Min, Yawei Luo, Wei Yang, Yuesong Wang, and Yi Yang. Entangled view-epipolar information aggregation for generalizable neural radiance fields. In *Proceedings of the IEEE/CVF Conference on Computer Vision and Pattern Recognition*, pages 4906–4916, 2024.
- [33] Michael Niemeyer, Jonathan T Barron, Ben Mildenhall, Mehdi SM Sajjadi, Andreas Geiger, and Noha Radwan. Regnerf: Regularizing neural radiance fields for view synthesis from sparse inputs. In *Proceedings of the IEEE/CVF Conference on Computer Vision and Pattern Recognition*, pages 5480–5490, 2022.
- [34] Christian Reiser, Rick Szeliski, Dor Verbin, Pratul Srinivasan, Ben Mildenhall, Andreas Geiger, Jon Barron, and Peter Hedman. Merf: Memory-efficient radiance fields for real-time view synthesis in unbounded scenes. *ACM Transactions on Graphics (TOG)*, 42(4):1–12, 2023.
- [35] Jeremy Reizenstein, Roman Shapovalov, Philipp Henzler, Luca Sbordone, Patrick Labatut, and David Novotny. Common objects in 3d: Large-scale learning and evaluation of real-life 3d category reconstruction. In *Proceedings of the IEEE/CVF international conference on computer vision*, pages 10901–10911, 2021.
- [36] Barbara Roessle, Jonathan T Barron, Ben Mildenhall, Pratul P Srinivasan, and Matthias Nießner. Dense depth priors for neural radiance fields from sparse input views. In *Proceedings of the IEEE/CVF Conference on Computer Vision and Pattern Recognition*, pages 12892–12901, 2022.
- [37] Mehdi SM Sajjadi, Henning Meyer, Etienne Pot, Urs Bergmann, Klaus Greff, Noha Radwan, Suhani Vora, Mario Lučić, Daniel Duckworth, Alexey Dosovitskiy, et al. Scene representation transformer: Geometry-free novel view synthesis through set-latent scene representations. In *Proceedings of the IEEE/CVF Conference on Computer Vision and Pattern Recognition*, pages 6229–6238, 2022.
- [38] Mohammed Suhail, Carlos Esteves, Leonid Sigal, and Ameesh Makadia. Generalizable patch-based neural rendering. In *European Conference on Computer Vision*, pages 156–174. Springer, 2022.
- [39] Mohammed Suhail, Carlos Esteves, Leonid Sigal, and Ameesh Makadia. Light field neural rendering. In *Proceedings of the IEEE/CVF Conference on Computer Vision and Pattern Recognition*, pages 8269–8279, 2022.
- [40] Cheng Sun, Min Sun, and Hwann-Tzong Chen. Direct voxel grid optimization: Super-fast convergence for radiance fields reconstruction. In *Proceedings of the IEEE/CVF conference on computer vision and pattern recognition*, pages 5459–5469, 2022.
- [41] Jingxiang Sun, Xuan Wang, Yong Zhang, Xiaoyu Li, Qi Zhang, Yebin Liu, and Jue Wang. Fenerf: Face editing in neural radiance fields. In *Proceedings of the IEEE/CVF conference on computer vision and pattern recognition*, pages 7672–7682, 2022.
- [42] Jia-Mu Sun, Tong Wu, and Lin Gao. Recent advances in implicit representation-based 3d shape generation. *Visual Intelligence*, 2(1):9, 2024.
- [43] Stanislaw Szymanowicz, Christian Rupprecht, and Andrea Vedaldi. Splatter image: Ultra-fast single-view 3d reconstruction. In *Proceedings of the IEEE/CVF Conference on Computer Vision and Pattern Recognition*, pages 10208–10217, 2024.
- [44] Hiroyuki Takeda, Sina Farsiu, and Peyman Milanfar. Image denoising by adaptive kernel regression. *Circuits Systems & Computers .conference Record.asilomar Conference on*, 2005, 2005.
- [45] Hiroyuki Takeda, Sina Farsiu, and Peyman Milanfar. Robust kernel regression for restoration and reconstruction of images from sparse noisy data. *IEEE*, 2006.
- [46] H. Takeda, S. Farsiu, and P. Milanfar. Kernel regression for image processing and reconstruction. *IEEE Transactions on Image Processing*, 2007.
- [47] Alex Trevithick and Bo Yang. Grf: Learning a general radiance field for 3d representation and rendering. In *Proceedings of the IEEE/CVF International Conference on Computer Vision*, pages 15182–15192, 2021.
- [48] Zhengzhong Tu, Hossein Talebi, Han Zhang, Feng Yang, and Yinxiao Li. Maxvit: Multi-axis vision transformer. *arXiv e-prints*, 2022.

- [49] Mukund Varma, Peihao Wang, Xuxi Chen, Tianlong Chen, Subhashini Venugopalan, and Zhangyang Wang. Is attention all that nerf needs? In *The Eleventh International Conference on Learning Representations*, 2022.
- [50] Ashish Vaswani, Noam Shazeer, Niki Parmar, Jakob Uszkoreit, Llion Jones, Aidan N Gomez, Łukasz Kaiser, and Illia Polosukhin. Attention is all you need. *Advances in neural information processing systems*, 30, 2017.
- [51] Naveen Venkat, Mayank Agarwal, Maneesh Singh, and Shubham Tulsiani. Geometry-biased transformers for novel view synthesis. *arXiv preprint arXiv:2301.04650*, 2023.
- [52] Can Wang, Menglei Chai, Mingming He, Dongdong Chen, and Jing Liao. Clip-nerf: Text-and-image driven manipulation of neural radiance fields. In *Proceedings of the IEEE/CVF Conference on Computer Vision and Pattern Recognition*, pages 3835–3844, 2022.
- [53] Dan Wang, Xinrui Cui, Septimiu Salcudean, and Z Jane Wang. Generalizable neural radiance fields for novel view synthesis with transformer. *arXiv preprint arXiv:2206.05375*, 2022.
- [54] Guangcong Wang, Zhaoxi Chen, Chen Change Loy, and Ziwei Liu. Sparsenerf: Distilling depth ranking for few-shot novel view synthesis. In *Proceedings of the IEEE/CVF International Conference on Computer Vision*, pages 9065–9076, 2023.
- [55] Qianqian Wang, Zhicheng Wang, Kyle Genova, Pratul P Srinivasan, Howard Zhou, Jonathan T Barron, Ricardo Martin-Brualla, Noah Snavely, and Thomas Funkhouser. Ibrnet: Learning multi-view image-based rendering. In *Proceedings of the IEEE/CVF conference on computer vision and pattern recognition*, pages 4690–4699, 2021.
- [56] Zhou Wang, Alan C Bovik, Hamid R Sheikh, and Eero P Simoncelli. Image quality assessment: from error visibility to structural similarity. *IEEE transactions on image processing*, 13(4):600–612, 2004.
- [57] Suttisak Wizadwongsa, Pakkapon Phongthawee, Jiraphon Yenphraphai, and Supasorn Suwajanakorn. Nex: Real-time view synthesis with neural basis expansion. In *Proceedings of the IEEE/CVF Conference on Computer Vision and Pattern Recognition*, pages 8534–8543, 2021.
- [58] Fanbo Xiang, Zexiang Xu, Milos Hasan, Yannick Hold-Geoffroy, Kalyan Sunkavalli, and Hao Su. Neutex: Neural texture mapping for volumetric neural rendering. In *Proceedings of the IEEE/CVF Conference on Computer Vision and Pattern Recognition*, pages 7119–7128, 2021.
- [59] Dejjia Xu, Yifan Jiang, Peihao Wang, Zhiwen Fan, Humphrey Shi, and Zhangyang Wang. Sinnerf: Training neural radiance fields on complex scenes from a single image. In *European Conference on Computer Vision*, pages 736–753. Springer, 2022.
- [60] Haofei Xu, Anpei Chen, Yuedong Chen, Christos Sakaridis, Yulun Zhang, Marc Pollefeys, Andreas Geiger, and Fisher Yu. Murf: Multi-baseline radiance fields. In *Proceedings of the IEEE/CVF Conference on Computer Vision and Pattern Recognition*, pages 20041–20050, 2024.
- [61] Tianhan Xu and Tatsuya Harada. Deforming radiance fields with cages. In *European Conference on Computer Vision*, pages 159–175. Springer, 2022.
- [62] Hao Yang, Lanqing Hong, Aoxue Li, Tianyang Hu, Zhen-guo Li, Gim Hee Lee, and Liwei Wang. Contranerf: Generalizable neural radiance fields for synthetic-to-real novel view synthesis via contrastive learning. In *Proceedings of the IEEE/CVF Conference on Computer Vision and Pattern Recognition*, pages 16508–16517, 2023.
- [63] Jiawei Yang, Marco Pavone, and Yue Wang. Freenerf: Improving few-shot neural rendering with free frequency regularization. In *Proceedings of the IEEE/CVF conference on computer vision and pattern recognition*, pages 8254–8263, 2023.
- [64] Alex Yu, Ruilong Li, Matthew Tancik, Hao Li, Ren Ng, and Angjoo Kanazawa. Plenotrees for real-time rendering of neural radiance fields. In *Proceedings of the IEEE/CVF International Conference on Computer Vision*, pages 5752–5761, 2021.
- [65] Alex Yu, Vickie Ye, Matthew Tancik, and Angjoo Kanazawa. pixelnerf: Neural radiance fields from one or few images. In *Proceedings of the IEEE/CVF conference on computer vision and pattern recognition*, pages 4578–4587, 2021.
- [66] Jason Zhang, Gengshan Yang, Shubham Tulsiani, and Deva Ramanan. Ners: Neural reflectance surfaces for sparse-view 3d reconstruction in the wild. *Advances in Neural Information Processing Systems*, 34:29835–29847, 2021.
- [67] Richard Zhang, Phillip Isola, Alexei A Efros, Eli Shechtman, and Oliver Wang. The unreasonable effectiveness of deep features as a perceptual metric. In *Proceedings of the IEEE conference on computer vision and pattern recognition*, pages 586–595, 2018.
- [68] Shunyuan Zheng, Boyao Zhou, Ruizhi Shao, Boning Liu, Shengping Zhang, Liqiang Nie, and Yebin Liu. Gps-gaussian: Generalizable pixel-wise 3d gaussian splatting for real-time human novel view synthesis. In *Proceedings of the IEEE/CVF Conference on Computer Vision and Pattern Recognition*, pages 19680–19690, 2024.
- [69] Tinghui Zhou, Richard Tucker, John Flynn, Graham Fyffe, and Noah Snavely. Stereo magnification: Learning view synthesis using multiplane images. *arXiv preprint arXiv:1805.09817*, 2018.
- [70] Haidong Zhu, Tianyu Ding, Tianyi Chen, Ilya Zharkov, Ram Nevatia, and Luming Liang. Caesarnerf: Calibrated semantic representation for few-shot generalizable neural rendering. In *European Conference on Computer Vision*, 2024.